Collective Binding Properties of Receptor Arrays

Noam Agmon and Arieh L. Edelstein
Department of Physical Chemistry and the Fritz Haber Research Center, The Hebrew University, Jerusalem 91904, Israel

ABSTRACT Binding kinetics of receptor arrays can differ dramatically from that of the isolated receptor. We simulate synaptic transmission using a microscopically accurate Brownian dynamics routine. We study the factors governing the rise and decay of the activation probability as a function of the number of transmitter molecules released. Using a realistic receptor array geometry, the simulation reproduces the time course of α-amino-3-hydroxy-5-methyl-4-isoxazolepropionic acid receptor-mediated excitatory postsynaptic currents. A consistent interpretation of experimentally observed synaptic currents in terms of rebinding and spatial correlations is discussed.

INTRODUCTION

The reversible binding of ligands (hormones, neurotransmitters) to an array of membrane-bound receptors is an important mechanism of intercellular communication. In particular, the mechanism of synaptic transmission has been extensively studied. Examples of important chemical synapses involve the nicotinic acetylcholine (ACh) receptor (Magleby and Stevens, 1972; Katz and Miledi, 1973) at the vertebrate neuromuscular junction (NMJ) and glutamate receptors (Eccles and Jaeger, 1958; Korn and Faber, 1991; Jonas and Spruston, 1994; Clements, 1996) in the central nervous system (CNS). Both have recently been reviewed (Edmonds et al., 1995a,b). The basic principles of operation are similar: the arriving presynaptic action potential triggers exocytosis of neurotransmitter-containing vesicles, and the agonist diffuses across the synaptic gap and binds reversibly to an array of receptors on the postsynaptic membrane. Apparently in all cases the binding of two transmitter molecules at two distinct subunits of the receptor protein triggers its ion channel opening (Patneau and Mayer, 1990; Clements and Westbrook, 1991). By monitoring the excitatory postsynaptic currents (EPSCs) through the receptor channels in the CNS or end-plate currents (EPCs) in the NMJ, receptor binding may be studied, albeit indirectly.

Although an analogy may be drawn between the response of ACh receptors at the NMJ and α-amino-3-hydroxy-5-methyl-4-isoxazolepropionic acid (AMPA) receptors in the CNS, there are also notable differences: 1) ACh is removed primarily by ACh esterase (AChE), whereas glutamate is removed by diffusion and reuptake; 2) AMPA receptors undergo notable desensitization (Patneau and Mayer, 1990; Vyklicky et al., 1991); 3) under typical conditions, the large receptor arrays at NMJ synapses are not saturated (Hartzell et al., 1975), whereas the smaller AMPA receptor arrays are likely to be saturated by a single vesicle ("quantum") of released neurotransmitter (Tang et al., 1994; Tong and Jahr, 1994).

The traditional view of synaptic transmission (Magleby and Stevens, 1972) is that diffusional aspects can be ignored because diffusion is fast on the EPSC time scale. The neurotransmitter (e.g. glutamate) has a brief residence time (1–2 ms) in the synaptic cleft (Clements et al., 1992; Clements, 1996). Exceptions, however, are documented. These include, in particular, the NMJ when transmitter clearance by AChE is blocked (Katz and Miledi, 1973; Hartzell et al., 1975; Magleby and Terrar, 1975; Kordaš, 1977; Land et al., 1984; Magazanik et al., 1984; Giniatullin et al., 1993) and glutamatergic CNS receptors with blocked desensitization (Yamada and Tang, 1993; Trussell et al., 1993; Barbour et al., 1994; Diamond and Jahr, 1995; Mennerick and Zorumski, 1995; Rossi et al., 1995; Takahashi et al., 1995). Thus to fully understand neurotransmission, the role of diffusion should be studied by theory and simulations. By applying a novel Brownian dynamics (BD) simulation technique, we will demonstrate how kinetic properties of receptor arrays may differ substantially from those of isolated receptors, even in the limit of fast diffusion.

In the NMJ, a multiquantal EPC decays more slowly than the smaller, single-quantum miniature EPC (Katz and Miledi, 1979). Under the influence of anti-AChE drugs, the EPC time course is prolonged (Katz and Miledi, 1973; Hartzell et al., 1975; Magleby and Terrar, 1975; Kordaš, 1977; Land et al., 1984; Magazanik et al., 1984; Giniatullin et al., 1993). Under these conditions, increasing the amount of transmitter released from the presynaptic terminal leads to further prolongation of EPCs (Magleby and Terrar, 1975) and mini-EPCs (Land et al., 1984). In response to paired stimuli, the second EPC is larger and slower, even when triggered during the tail of the first EPC (Magazanik et al., 1984). Even with AChE intact, multiquantal EPCs are prolonged when the number of quanta exceeds a certain critical value (Giniatullin et al., 1993). For large concentrations of transmitter, reduction in postsynaptic receptor density (e.g., by α-bungarotoxin) enhances EPC decay (Katz and Miledi, 1973; Land et al., 1984; Giniatullin et al., 1993). These findings are generally in agreement with the hypothesis of

Received for publication 24 October 1996 and in final form 10 January 1997.

Address reprint requests to Dr. Noam Agmon, Department of Physical Chemistry, Fritz Haber Research Center, The Hebrew University, Jerusalem 91904, Israel. Tel.: 972-2-6585687; Fax: 972-2-6513742; E-mail: agmon@batata.fh.huji.ac.il.

0006-3495/97/04/1582/13 $2.00

Katz and Miledi (1973), that a fundamental determinant of EPC decay in the absence of AChE is repetitive binding of neurotransmitter molecules. However, the precise dependence on the number of released transmitter molecules seems more complex to interpret.

In mature CNS synapses, AMPA receptors are responsible for most of the EPSC amplitude, with about 10% of the amplitude carried by the slower *N*-methyl-D-aspartate (NMDA) receptor channels, apparently colocalized on the same receptor array (Bekkers and Stevens, 1989). Studies of NMDA receptors ruled out glutamate rebinding in shaping the EPSC decay (Lester et al., 1990). One review cites six pieces of evidence favoring deactivation of NMDA-receptor in shaping the EPSC decay (Jonas and Spruston, 1994). These studies have created the impression that repetitive binding (Katz and Miledi, 1973) is unimportant in the CNS in general (Jonas and Spruston, 1994; Clements, 1996). The simulations reported below, and several recent experimental observations, indicate that this might not be true for AMPA receptors under certain conditions.

The elementary AMPA receptor deactivation step observed in outside-out patch-clamp experiments may be as short as 1 ms (Yamada and Tang, 1993). Miniature EPSC decay in small cerebellar granule cells reaches this lower limit, consistent with individual open times recorded from these cells (Silver et al., 1992). Most hippocampal neurons exhibit slower EPSC decay, 2–3 ms (Jonas and Spruston, 1994), slower than typical open times in these cells (Yamada and Tang, 1993). Even EPSCs from the small granule cells were recently observed to decay more slowly than single-receptor deactivation and to exhibit a second slow decay phase (Silver et al., 1996). In addition, large evoked EPSCs decayed more slowly than the smaller spontaneous EPSCs (Silver et al., 1996). In some giant synapses a slow component of EPSC decay has been observed to last for several seconds (Rossi et al., 1995). Thus there seems to be a correlation between a synapse size and its EPSC amplitude and decay time. The heterogeneity in hippocampal synaptic size might explain the heterogeneity of synaptic efficacy (Lisman and Harris, 1993).

Furthermore, block of desensitization with cyclothiazide (CTZ) unmasks a slow decay phase of several dozen milliseconds (Yamada and Tang, 1993; Trussell et al., 1993; Diamond and Jahr, 1995; Mennerick and Zorumski, 1995; Takahashi et al., 1995). After CTZ treatment, block of glutamate uptake can further prolong the evoked response (Mennerick and Zorumski, 1995). In Purkinje cells, uptake block prolongs the response even without block of desensitization (Barbour et al., 1994; Takahashi et al., 1995). In some cases a very slow EPSC decay component, selectively increased and prolonged by uptake block, is clearly identifiable even without blocking desensitization (Otis et al., 1996). Prolongation of EPSC decay was ascribed to various microscopic mechanisms, either slow diffusional clearance and repetitive binding (Barbour et al., 1994; Mennerick and Zorumski, 1995; Rossi et al., 1995; Otis et al., 1996; Silver et al., 1996) or asynchrony in the presynaptic exocytosis process (Diamond and Jahr, 1995; Isaacson and Walmsley, 1995).

The mechanistic differences cannot be settled by homogeneous chemical kinetics (Rosenberry, 1979; Wathey et al., 1979; Parnas et al., 1989) or approximate diffusion treatments (Friboulet and Thomas, 1993; Holmes, 1995; Uteshev and Pennefather, 1996; Kleinle et al., 1996). These ignore one or more of the following aspects: the geometric confinement of receptors and transmitter molecules between two membranes, the static distribution of receptors on one of these membranes, and the initial inhomogeneous distribution of transmitters with their subsequent diffusion and their individual identity, only approximately describable by bulk concentrations. The chemical kinetic approaches assume that receptors and transmitters are homogeneously mixed in solution, eliminating geometric effects that might arise from the narrow synaptic gap and the spatial proximity of the static receptors. Approximate diffusion approaches solve a diffusion equation uncoupled from reversible binding, then use the calculated concentration profile to "drive" a kinetic scheme. In all approaches utilizing macroscopic concentrations the notion of rebinding is undefined because the history of individual transmitter molecules cannot be monitored.

A microscopic picture of reversible binding can be obtained from computer simulations. A few Monte Carlo simulations have been reported (Bartol et al., 1991; Faber et al., 1992; Wahl et al., 1996). The present study will investigate the determinants of synaptic currents using a novel Brownian simulation technique. Aside from the fact that reversible binding is treated more accurately in the present BD algorithm (Agmon and Edelstein, 1995; Edelstein and Agmon, 1997), there is a basic change in philosophy. Existing simulations involve a receptor kinetic scheme to which diffusion was added. Our approach is to incorporate the fundamental morphological details without introducing receptor substates.

The simulations provide us with a wealth of detailed information, from the transient development of individual receptor binding states ("excitation patterns") to the average fraction of activated receptors. Although we find that neurotransmitter diffusion in the synaptic cleft is an order of magnitude slower than in water, it is still fast. Diffusion in the liquid phase affects mainly the rising phase of the activation probability. The decay is governed by an effective "surface diffusion" of transmitter molecules hopping between binding sites on the receptor array. This process depends in a nontrivial way on the "coverage" (degree of saturation) of the array and the spatial correlation between receptors. Finally, we are able to reproduce an AMPA receptor-mediated EPSC with physically realistic binding and geometric parameters.

METHODS

We have developed a computer program (Agmon and Edelstein, 1995; Edelstein and Agmon, 1997) for simulating

many-particle reversible binding to a receptor array (Fig. 1). The system consists of two parallel, inert and impermeable membranes between which noninteracting transmitter particles (agonist) diffuse with a diffusion coefficient D. The "ceiling" (top) and "floor" (bottom) of the simulation box represent the pre- and postsynaptic membranes, respectively. Their separation (in the z direction) is L. N transmitter particles are released at time $t = 0$ from the center of the ceiling. In the "chessboard approximation" (Fig. 1), the floor is covered by M square tiles (binding sites of length l) arranged as an $m \times m$ array ($M = m^2$). Here l determines both the distance between binding sites and their area, $a = l^2$. This simple geometry is useful for theoretical analysis. When comparing with experiment, l is replaced by three different distances: the size of the binding site, the distance between sites within a receptor, and the distance between receptors. Each site may bind at most one transmitter molecule, and either one or two sites constitute a receptor (a double-site receptor is probably the experimental case; Patneau and Mayer, 1990). When a particle touches the site's surface, binding may occur with a rate coefficient $a\kappa_r$, provided that it is unoccupied (κ_r is the reactive flux perpendicular to the site surface). If a particle is bound, the site becomes inert. The bound particle may in turn dissociate to an arbitrary point on the surface with a rate coefficient κ_d. Thus the site affinity constant is

$$K_d \equiv \kappa_d/(a\kappa_r). \quad (1)$$

It can be determined experimentally, e.g., from dose-response relationships (Patneau and Mayer, 1990).

Either the simulation box is enclosed within walls ($+W$), so that the whole floor is a receptor array, or the membranes stretch indefinitely in the x-y directions ($-W$). In the first case, the total number of bound particles increases monotonically to equilibrium as the concentration of bound plus unbound particles within the volume $V = LMl^2$ tends to $c \equiv N/V$. Study of the $-W$ case allows one to follow the decay phase of transmitter clearance by diffusion. The program utilizes intrinsic time units (tu) and distance units (du), in which $D = 1$ du^2/tu and $\kappa_r = 1$ du/tu. This leaves L, l, N, m, and κ_d to be varied for the chessboard approximation. We subsequently determine tu by fitting the EPSC shape and du from the experimental K_d value. This provides a physical distance scale for all other geometric parameters.

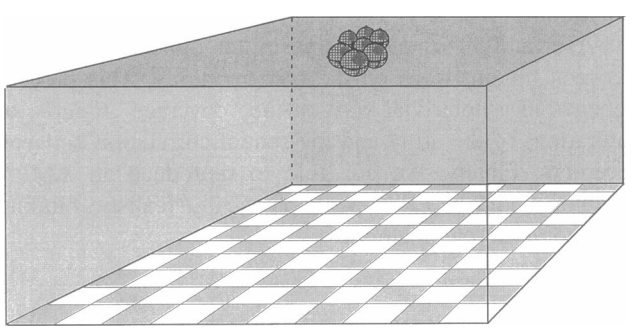

FIGURE 1 The model receptor array simulated in the chessboard approximation.

The numerical algorithm is an extension of our one-dimensional many-body BD algorithm for reversible binding (Edelstein and Agmon, 1993, 1995; Agmon and Edelstein, 1995): a particle is chosen at random and moved along x and y using two Gaussian random numbers. However, along z (perpendicular to the array) we apply a random number from the exact one-dimensional solution of diffusion near a reversible trap, using a fast lookup table procedure. In addition, we apply geometry-sensitive time steps. These two measures make it possible to take relatively large time steps, without sacrificing numerical accuracy. The algorithm is summarized in detail elsewhere (Edelstein and Agmon, 1997).

During a stochastic trajectory, the program retains information on the spatial location of each particle, $x_i(t)$, $y_i(t)$, and $z_i(t)$, $i = 1, \ldots, N$, as a function of time, t. Knowledge of whether particle i is in the intermembranal solution or bound to site j makes it possible to construct the binding state of each site, $P_j(t)$, $j = 1, \ldots, M$. In a given trajectory, $P_j(t)$ is either 0 (unbound) or 1 (bound), giving rise to spatiotemporal "excitation patterns." When averaged over many (10–10,000) trajectories, we obtain the individual-site binding probabilities $\langle P_j(t)\rangle$. Summing over all sites gives the total binding (or "activation") probability for single-site receptors, $\langle P(t)\rangle \equiv 1/M \sum_{j=1}^{M} \langle P_j(t)\rangle$. Thus $M\langle P(t)\rangle$ is the average number of bound particles and $M\langle P(t)\rangle/N$ is the fraction of bound particles per the total (bound plus free) particles. For double-site receptors one calculates $\langle P(t)\rangle_{(2)}$ (instead of $\langle P(t)\rangle$) by counting only odd-numbered sites, j, *provided* that $j + 1$ is bound. Hence only simultaneously bound pairs contribute to $\langle P(t)\rangle_{(2)}$, which is assumed to be proportional to the macroscopic ionic current through the postsynaptic channels. We check whether this assumption is plausible by fitting experimental EPSC data below.

THE CHESSBOARD APPROXIMATION

Let us first investigate the qualitative determinants of EPSCs within the simplified "chessboard approximation." The parameters used in our 10×10 chessboard simulations are summarized in Table 1. They are such that the dissociation time, $1/\kappa_d$, is intermediate between the transversal (perpendicular) and longitudinal (parallel to the array) diffusion times. The initial distribution is a delta function at the center of the "ceiling." Fig. 2 summarizes several aspects of the overall activation probability for single-site receptors. Although the $\pm W$ cases are expected to differ only marginally during the rising phase, the introduction of walls imposes an

TABLE 1 Parameters used in the simulations under the chessboard approximation

L (du)	l (du)	N	m	κ_d (1/tu)	Walls
10	10	10, 100	10	0.01, 0.1	+, −

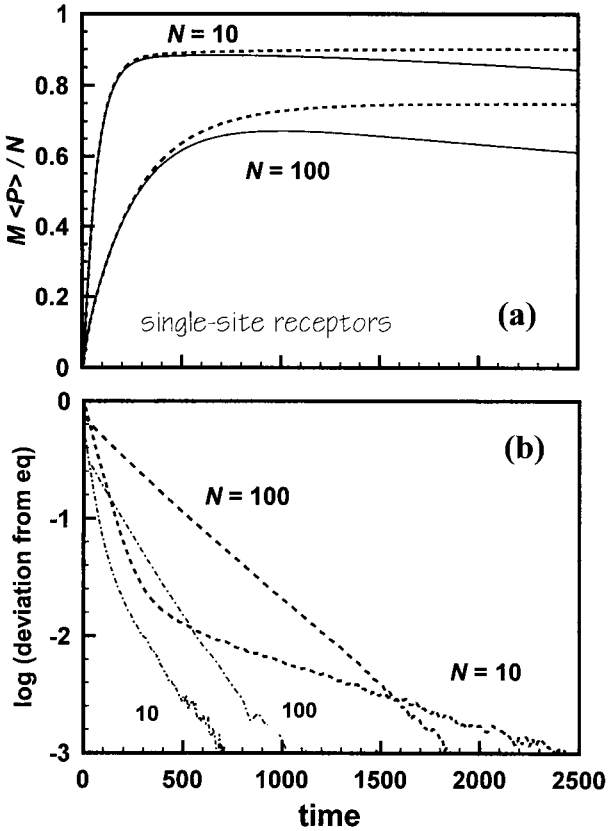

FIGURE 2 Averaged total binding probabilities in the chessboard approximation for two values of N and of κ_d (other parameters in Table 1). (*a*) The fraction of bound particles for $\kappa_d = 0.01$ with (– – –) and without (——) walls. (*b*) $M[P_{eq} - \langle P(t)\rangle]/N$ on a semilog scale for $+W$ $\kappa_d = 0.01$ (– – –) and $+W$ $\kappa_d = 0.1$ (– · –).

ultimate equilibrium solution, $P_{eq} \equiv \langle P(\infty)\rangle$, which serves as a check of the computer program.

The dashed curves in Fig. 2 *a* show the $+W$ fraction of bound particles as a function of time. We observe that the "deviation from equilibrium" (Fig. 2 *b*) decays either mono- or biexponentially:

$$P_{eq} - \langle P(t)\rangle \approx P_{eq}[A_0 \exp(-t/\tau_0) + (1 - A_0)\exp(-t/\tau_1)]. \quad (2)$$

The parameters P_{eq}, τ_0, A_0, and τ_1 are collected in Table 2. Although we derive an analytic expression for P_{eq}, we can currently offer only a qualitative discussion of the two decay times.

The equilibrium limit

For a single site ($M = 1$) at equilibrium (Agmon and Szabo, 1990),

$$P_{eq} = c/(K_d + c). \quad (3)$$

A second site encounters a lower concentration of free particles, leading to smaller P_{eq}. As demonstrated in Table 2, Eq. 3 is indeed an upper bound, which becomes exact only when $M = 1$ or $N \to \infty$.

TABLE 2 Approach to equilibrium for a receptor array with walls

N	P_{eq}	Eq. 3	Eq. 4	τ_0 (tu)	A_0	τ_1 (tu)
10	0.090	0.333	0.091	740	0.026	65
100	0.736	0.909	0.733	300	0.85	65?

Parameters from fitting Eq. 2 to the kinetics in Fig. 2 *b* for $\kappa_d = 0.01$ tu^{-1}.

To obtain the exact many-particle equilibrium binding probability, we replace c with the concentration of free particles, $c_f \equiv [N - (M - 1)P_{eq}]/V$. This produces a quadratic equation for P_{eq},

$$(M - 1)P_{eq}^2 - (VK_d + N + M - 1)P_{eq} + N = 0. \quad (4)$$

Its solutions (Table 2) agree nicely with the simulation to within its numerical accuracy ($\sim \pm 0.003$). This demonstrates both the accuracy of the simulation and the correctness of Eq. 4.

The rising phase

The rising phase is nearly identical in the $\pm W$ cases (Fig. 2 *a*). The rate of approaching equilibrium in the $+W$ case (Fig. 2 *b*) may involve processes that shape both the rise and early decay phases in the $-W$ case. Table 2 shows two interesting effects of varying N on the exponents of Eq. 2: 1) the slow exponent, τ_0, decreases with increasing N; and 2) for small N the fast exponent, τ_1, becomes dominant (small A_0). As a result, the rising phase is considerably faster for 10 particles as compared with the 100-particle case.

What is the origin of the two exponents and their N dependence? Transmitter molecules initially bind to the central sites opposing the release site. Hence for small N the rise time is determined by transversal diffusion, giving rise to the fast exponent, τ_1. For large N, the whole array is involved in the initial binding step. Therefore, the time to peak corresponds to the lateral diffusion time, τ_0, which depends on N as discussed below.

The effects of varying N and κ_d on τ_0 may be interpreted as being due to retardation of lateral diffusion induced by repetitive binding. This effect should be larger 1) for small N, when most of the sites are free, and 2) for small κ_d, when release from an individual site is slower.

In these limits τ_0 should be most sensitive to variation in these parameters. Indeed, when κ_d is increased from 0.01 to 0.1, τ_0 decreases and becomes independent of N (Fig. 2 *b*). More quantitatively, repetitive binding is an effective two-dimensional "hopping" between vacant sites, with an effective diffusion coefficient $D_{eff} = l^2\kappa_d$. For $\kappa_d = 0.01$, $D_{eff} = D = 1$. For $\kappa_d = 0.1$, $D_{eff} > D$, so that repetitive binding, which still occurs, does not delay transmitter clearance.

The assignment of τ_1 to transversal diffusion is corroborated by the individual-site activation probabilities in Fig. 3. Note that whereas $\langle P(t)\rangle$ increases monotonically to equilibrium, $\langle P_j(t)\rangle$ may go through a maximum, even in the

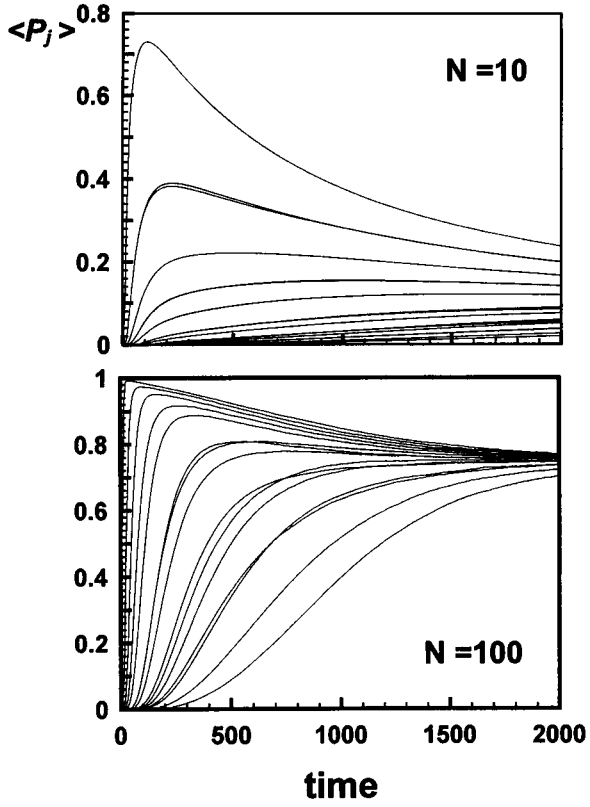

FIGURE 3 Average binding probabilities for individual sites. $\kappa_d = 0.01$, $+W$ (during the rising phase there are only small differences between the $\pm W$ cases). There are 100 sites arranged with fourfold symmetry around the release site. By symmetry, there are only 15 different kinetic behaviors. The largest binding probability is that of the four binding sites directly under the release site ($j = 1 - 4$), and the smallest signal comes from the four sites at the corners of the array. The remaining kinetic traces (*top to bottom*) are ordered more or less by their distance from the release site.

absence of clearance processes. The peak is most pronounced for "central sites" ($j \approx 1$), located just beneath the release site. Peripheral sites show only a mild peak if any, with a significantly slower rise time than the central receptors. $\langle P_1(t) \rangle$ for $N = 10$ reaches 95% of its peak by time $\tau_1 = 65$ tu. Here central sites carry most of the signal, so that their kinetics indeed determines the overall risetime. For $N = 100$, the peak in $\langle P_j(t) \rangle$ occurs at shorter times, because more particles compete for binding. However, this time is of little relevance for the overall EPSC risetime, since now also the peripheral sites contribute to the observed signal.

The single trajectories ("excitation patterns") in Figs. 4 and 5 demonstrate that τ_1 and τ_0 are indeed the characteristic times for transversal and lateral diffusion. For small N (Fig. 4) the risetime is dominated by transversal diffusion. During this initial phase, diffusion is hemispheric in three dimensions (Gutman et al., 1992). As diffusion covers an average distance L perpendicular to the membrane, all sites within a "disk" of radius L on the postsynaptic membrane become occupied. From Fig. 4 and $L = l$ one concludes that $\tau_1 \approx 60$ tu, in agreement with our conclusion from Fig. 3.

Consider next the transversal diffusion time τ_0. For $t > \tau_1$ diffusion becomes effectively two dimensional (Gutman et al., 1992) and τ_0 is determined by the time to reach the boundary of the array. For $N = 10$ (Fig. 4), an occupied boundary site is first found by time $t = \tau_0 = 700$ tu, whereas for $N = 100$ (Fig. 5) several occupied peripheral sites are first observed by $\tau_0 = 300$ tu. These numbers agree nicely with those of Table 2. τ_0 is long for $N = 10$, because of repetitive binding, and brief for $N = 100$, where high surface coverage prevents the remaining particles from rebinding. The difference in τ_0, 400 tu, corresponds to four binding cycles with a delay of $1/\kappa_d = 100$ tu each. It follows that the rising phase, which is dominated by τ_1 for small N and τ_0 for large N, is actually hardly affected by repetitive binding.

It is amusing to consider in more detail the development of the excitation patterns. Particles start binding at the center of the array, closest to the release site, after a short delay due to transversal diffusion. When N is large, a compact island grows. The growing mechanism is similar to that of Eden clusters on surfaces (Becker et al., 1990), where particles diffuse on top of the adsorbed layer. Here particles that cannot bind to occupied sites diffuse laterally in the liquid gap until they reach the rim of the island, where they land. Up to $t \approx 1/\kappa_d = 100$ tu particles bind irreversibly: new ones are added without desorption of previously bound particles. At $t = 200$ tu, the first dissociation event occurs. For large N, holes are formed in the compact island, leading to a transition to percolation-like patterns. It might be interesting to monitor such patterns experimentally (Gogan et al., 1995).

Amplitude–rise time correlations

For both NMJ ACh receptors (Land et al., 1981) and CNS glutamatergic receptors (Mennerick and Zorumski, 1995; Silver et al., 1996), a faster rise time sometimes correlates with smaller synaptic currents. In the NMJ the correlation becomes more prominent as the receptor surface density is reduced by α-bungarotoxin (Land et al., 1981). This correlation was explained with the "saturated disk model" (Land et al., 1981): the N released transmitter molecules were assumed to saturate a disk of neurotransmitters under the release site. The diffusion time across the disk is proportional to its area and hence to N, and hence to the EPC amplitude. This explained the positive correlation between rise time and amplitude.

Our simulations confirmed the saturated disk hypothesis only for times shorter than the dissociation time; for $t > 1/\kappa_d$ the compact "island" of bound receptors beneath the release site is destroyed (Figs. 4 and 5). Although we do find a correlation between the rise time and N (Fig. 2), its origin is different. First, the longitudinal diffusion time τ_0 is the time to cross the whole array rather than just the island of bound receptors. It actually decreases with increasing N because of reduced repetitive binding. Therefore, longitu-

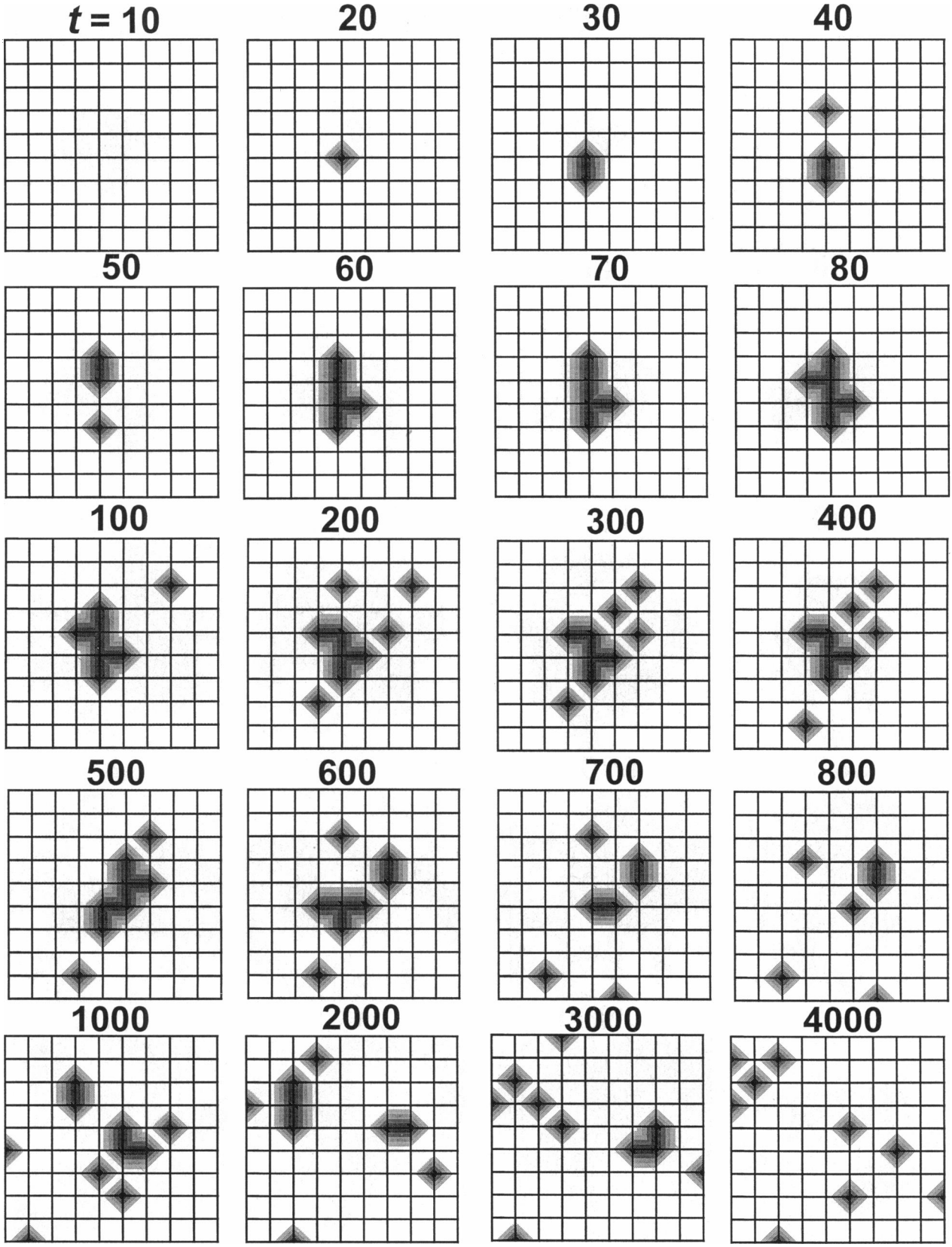

FIGURE 4 A single trajectory depicting transient binding states for $N = 10$, $\kappa_d = 0.01$, and $+W$. The 20 time frames represent a "movie" describing the temporal evolution of the binding states. Each frame portrays the 10×10 receptor array with bound particles marked as small diamonds. The bound sites form an "excitation pattern" in two dimensions.

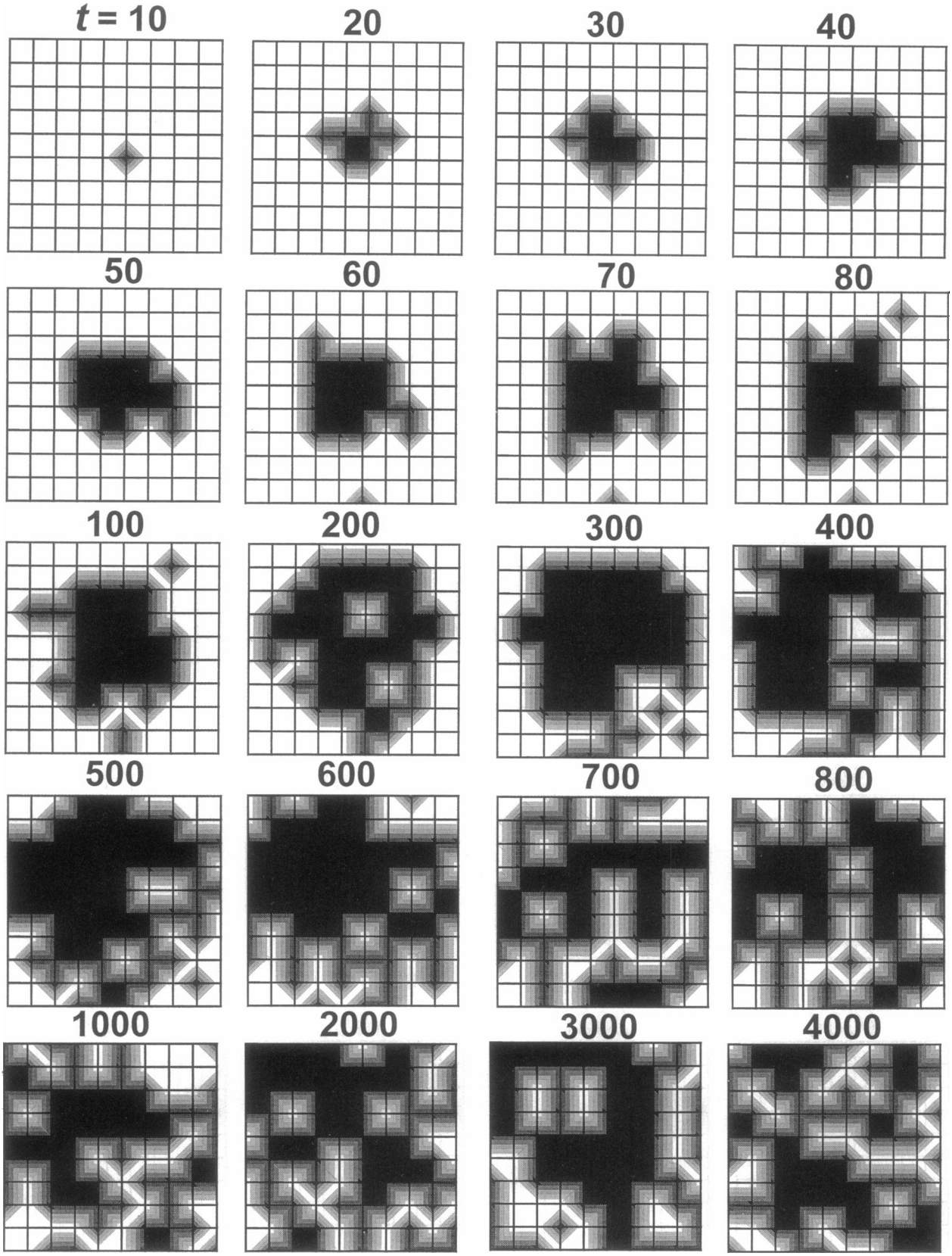

FIGURE 5 A single trajectory for $N = 100$ particles. Other details are as in Fig. 4.

dinal diffusion alone does not explain the correlation. Second, we find that for small N the rise time is dominated by the fast three-dimensional transversal diffusion time, τ_1. In our simulations the increase in rise time with increasing N therefore reflects a "change in mechanism": it is controlled by τ_1 for small N and by the slower τ_0 for large N.

The decay phase

Whereas repetitive binding has little effect on the rising phase, the situation is different for the $-W$ decay phase, provided that additional factors, such as AChE and desensitization, are inoperative. When the array is saturated, no rebinding occurs and transmitter molecules are cleared rapidly by diffusion in the liquid phase. At later times and under low coverages, transmitter clearance is delayed substantially by repetitive binding. Thus when $D_{\text{eff}} \leq D$ and N large, we expect a range of transmitter clearance times, making the fraction of bound particles, $M\langle P\rangle/N$, decay nonexponentially. In particular, its initial decay should be faster for large N because of elimination of repetitive binding, as demonstrated by the solid lines in Fig. 2 *a*.

So far we have considered the total occupancy of the array irrespective of the number of binding sites per receptor. Interestingly, the situation is reversed for the activation probability of double-site receptors because of the enhancement of nearest-neighbor correlations with increasing N. Suppose that only one receptor in the array is doubly occupied. Any dissociation event, followed by recombination to a different site, creates two inactive, singly occupied receptors. At higher coverages, the rebinding particle may land in a singly occupied receptor, converting it to the doubly occupied, active state. Hence slower decay is expected for larger N, just the opposite of the behavior for singly occupied receptors. This prediction is confirmed in Fig. 6. In the NMJ, smaller miniature EPCs decay faster than larger EPCs (Katz and Miledi, 1979), and, under the influence of anti-AChE, the EPC is prolonged with increased transmitter release (Magleby and Terrar, 1975).

As Fig. 6 shows, the initial fast decay might be described as an exponential, $\exp(-t/\tau_f)$, but the tail is better fitted to a hyperbola:

$$\langle P(t)\rangle_{(2)} \sim [B_0 + B_1 t]^{-1}. \tag{5}$$

The parameters τ_f, B_0, and B_1 are collected in Table 3. It is seen that for small N, the slower rise-time phase is similar to the fast decay phase, $\tau_0 \approx \tau_f$. It is considerably slower than the transmitter dissociation time, $1/\kappa_d$, due to repetitive binding. For large N, τ_f becomes even slower and then $\tau_f \ll \tau_0$.

That the long-time tail is better described by a hyperbola than a second exponent is evident from the semilogarithmic plot (Fig. 6 *b*). For a geminate (receptor-agonist) pair in two dimensions, theory predicts an asymptotic decay of $1/(4\pi K_d t)$ (Agmon and Szabo, 1990). In the present example, $4\pi\kappa_d/(a\kappa_r) \approx 1.26 \times 10^{-3}$ tu^{-1}. This is rather close to the values of B_1 in Table 3. The precise theoretical asymptotic behavior for a whole array is unknown. It would be interesting if EPSC tails could be measured sufficiently accurately to determine whether they are exponential or hyperbolic.

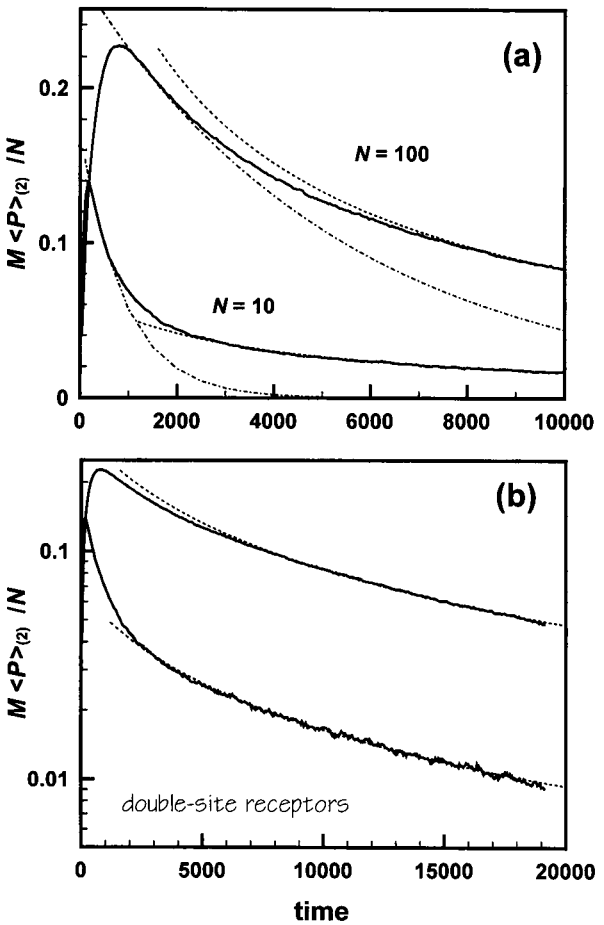

FIGURE 6 Activation probabilities for double-site receptors (without walls) as a function of the number of transmitter molecules released, N. Same conditions as in Fig. 2 and $\kappa_d = 0.01$. Dash-dotted and dashed lines are fits of the initial and long-time decay to exponential and hyperbolic functions, respectively, with parameters collected in Table 3. (*a*) linear and (*b*) semilogarithmic scales.

A REALISTIC SIMULATION OF AMPA EPSC

After the qualitative analysis of EPSC characteristics, it is natural to ask whether the simulation can explain some data quantitatively. AMPA receptors account for most of the excitatory synaptic transmission in the CNS. Their rising phase is usually fast, sometimes unresolved, and possibly convoluted by details of the release process (location of

TABLE 3 Parameters for the exponential and hyperbolic fits to the decay phase of double-site receptors (Fig. 6)

N	τ_f (tu)	B_0	B_1 (tu^{-1})
10	900	15	$4.6 \cdot 10^{-3}$
100	5500	3	$9 \cdot 10^{-4}$

release sites, asynchrony of release; Diamond and Jahr, 1995; Isaacson and Walmsley, 1995). Their decay is complicated by rapid desensitization (Patneau and Mayer, 1990; Yamada and Tang, 1993). Therefore we fit the decay phase of EPSCs from CTZ-treated cells. CTZ inhibits AMPA-receptor desensitization (Vyklicky et al., 1991; Yamada and Tang, 1993; Trussell et al., 1993), thus revealing the inherent kinetic properties of the receptor array.

The experimental situation is approximated by the $-W$ case (walls removed) and double-site receptors. In addition, we extend our model beyond the "chessboard approximation" in which a single distance, l, governed both inter and intrareceptor distances. This parameter is replaced by three characteristic distances: l is now the microscopic length of a square binding site. Each site occupies the center of a nonreactive l'_x by l'_y rectangle. Two adjacent sites (distance l'_x) are coupled along x to form a single receptor. Hence $2l'_x$ and l'_y are the distances between receptor centers along x and y, respectively. We still apply a delta-function initial condition, although this detail is probably unimportant for the decay phase, which is preceded by near-saturation of the array.

Our model involves the nine geometric and kinetic parameters listed in Table 4, considerably less than in conventional approaches utilizing multiple receptor substates (Holmes, 1995; Table 1). Fitting the experiment by systematically varying each of these parameters is prohibitively time-consuming. It is also unnecessary, because two of the parameters (e.g., D and κ_r) set the time and distance scales. In our approach, the array geometry is set on a relative distance scale using intrinsic distance units (du). For various κ_d and N values, the simulation is run using intrinsic time units (tu). If the EPSC shape can be reproduced by scaling the time axis, we get a possible determination of tu. To set du, we require that K_d of Eq. 1 agrees with the experimental affinity constant (Patneau and Mayer, 1990).

With sustained agonist application, AMPA currents desensitize rapidly to a steady-state (SS) value (Patneau and Mayer, 1990; Yamada and Tang, 1993). K_d (and EC_{50}) are considerably larger for the peak as compared with the SS response. For glutamate, the values are about 500 and 9 μM, respectively (Patneau and Mayer, 1990). With the application of CTZ, the transient peak disappears, and the peak response EC_{50} (measured for quisqualate and kainate) tends to the lower SS value (Yamada and Tang, 1993; Patneau et al., 1993). Thus, in addition to elimination of desensitization, the receptor affinity increases, partly because of slower deactivation (Patneau et al., 1993). Presumably, in the presence of CTZ, K_d assumes its SS value also for glutamate (9 μM; Patneau and Mayer, 1990; Table 2). We use this value to set the distance scale for the simulation.

A fit to the decay phase of CTZ-treated AMPA-mediated EPSC (Diamond and Jahr, 1995) (Table 1) is shown in Fig. 7. The parameters are summarized in Table 4, using both intrinsic and physical units. The ensuing distances are physically reasonable: a binding site of length 4 Å, a synaptic-gap width of 12 nm; each receptor occupies $2l'_x\, l'_y = 55$ nm^2, corresponding to a surface density of 18,500 receptors/μm^2. The latter value is intermediate between a particle density of 3000/μm^2 counted in freeze-fractured preparations from rat hippocampus (Harris and Landis, 1986) and about 25,000 receptors/μm^2 found in the frog NMJ (Matthews-Bellinger and Salpeter, 1978).

The diffusion coefficient emerging from our fitting procedure (7×10^{-7} cm^2/s) is an order of magnitude smaller than that of glutamic acid in water (7.6×10^{-6} cm^2/s; Longworth, 1953). The diffusion of ions in the extracellular

TABLE 4 Kinetic and geometric parameters in fitting the AMPA-receptor EPSC decay (Fig. 7) in intrinsic time and distance units (tu and du) and physical units

Parameter	Intrinsic units	Physical units
κ_r	1 du/tu	0.82 nm/ns
κ_d	$7.5 \cdot 10^{-8}$ tu^{-1}	0.75 ms^{-1}
D	1 du^2/tu	$7 \cdot 10^{-7}$ cm^2/s
l	5 du	0.4 nm
l'_x	40 du	3.3 nm
l'_y	100 du	8.2 nm
L	150 du	12 nm
m	15	15
N	1000	1000

1 tu = 0.1 ns (from fitting Fig. 7) and 1 du = 0.082 nm (from requiring that K_d = 9 μM; Patneau and Mayer, 1990). The time step in this simulation was 20,000 tu = 2 μs.

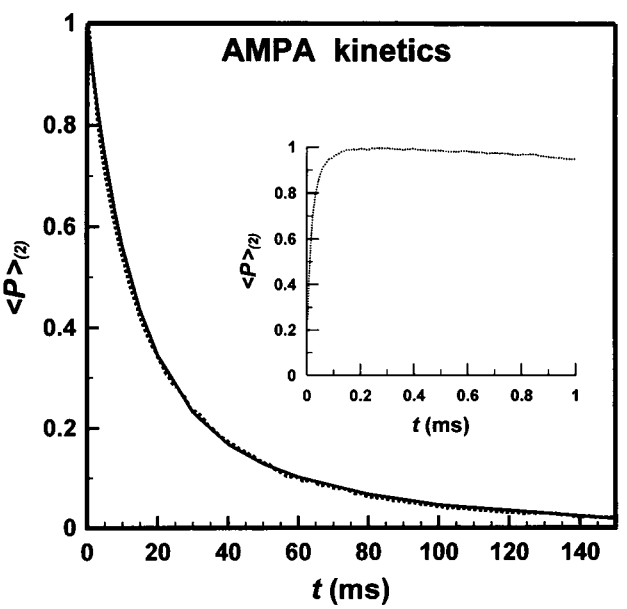

FIGURE 7 AMPA receptor-mediated EPSC in CTZ-treated rat hippocampal neurons. ——, Experimental data (Diamond and Jahr, 1995) fitted to a biexponential, 0.71 exp($-t$/12.6) + 0.29 exp($-t$/54.1), t in ms. – – –, Activation probabilities from $-W$ simulations of a 15 × 15 array of binding sites, coupled into 112 double-site receptors. Simulation parameters are in Table 4. (*Inset*) Simulated rising phase, with a peak around 300 μs corresponding to 98% saturation. The initially unbound particles (about 780 out of 1000) clear the gap within this time scale. The remaining particles undergo multiple binding cycles.

space within the brain has been measured to be slower than in solution by a factor of 3 (Nicholson and Phillips, 1981; Rice et al., 1985). It is possible that diffusion is attenuated by an additional factor of 3 in the synaptic cleft. This agrees with electron microscopy data showing that the cleft includes many structural elements that may physically impede diffusion (Ichimura and Hashimoto, 1988). One study even reports diffusion coefficients for cations in the extracellular space that are smaller by a factor of 10 than in solution (Rice et al., 1985). Our factor of 10 is also in agreement with the conclusion of a recent theoretical estimate (Kleinle et al., 1996).

The simulations indicate that $N = 1000$ is sufficient to produce saturation at the EPSC peak. A further increase in N will not alter the decay phase, because by the peak's time excess transmitter particles have already cleared the synaptic cleft. Thus even if a single synaptic vesicle contains more (a few thousand) particles, our results are not expected to change. It is interesting, however, that our simulation predicts saturation of the AMPA receptor array, in agreement with (indirect) experimental evidence (Tang et al., 1994; Tong and Jahr, 1994) and in contrast to approximate diffusion equation solutions (Holmes, 1995). It is also interesting that, for the present parameter set (and in contrast to the previous section), decreasing N to below saturation enhances the decay rate only slightly. This might relate to the suggestion that, in contrast to ACh receptors in the NMJ, in glutamatergic CNS receptors variation in EPSC response is primarily connected to variations in size of the postsynaptic receptor array (Lisman and Harris, 1993).

Most interesting for our interpretation is $\kappa_d = 0.75\ \text{ms}^{-1}$, implying that a transmitter molecule dissociates about once every millisecond. This agrees with the 1-ms decay of spontaneous miniature EPSCs observed in some cerebellar synapses (Silver et al., 1992) and the <2-ms deactivation times recorded from single channels in outside-out patches from rat hippocampus (Yamada and Tang, 1993). Thus the elementary dissociation event is considerably faster than the EPSC decay of Fig. 7. Consequently, multiple dissociation-recombination cycles occur during the decay phase. This is corroborated by single-trajectory excitation patterns (not shown): by following the history of individual transmitter particles we observe that some of them rebind dozens of times before escaping from the array.

It is appropriate to mention here the difference between the microscopic rate coefficients, κ_d and κ_r, and the steady-state "off" and "on" rate parameters. The latter also include the effect of diffusion. The diffusion rate coefficient for a cubic binding site of length l may be approximated by

$$k_D \approx 2Dl. \tag{6}$$

This approximation is modeled after the exact expression for a reactive disk of radius r, which is $4Dr$ (Shoup and Szabo, 1982). For an approximate three-step kinetic scheme for agonist (A) receptor (R) binding,

$$A + R \underset{k_D}{\overset{k_D}{\rightleftharpoons}} A \cdots R \underset{\kappa_d}{\overset{a\kappa_r}{\rightleftharpoons}} RA, \tag{7}$$

a steady-state assumption of the intermediate "contact pair," $A \cdots R$, gives

$$k_{on} = k_D\, a\kappa_r/(k_D + a\kappa_r)$$
$$k_{off} = k_D\, \kappa_d/(k_D + a\kappa_r). \tag{8}$$

The equilibrium (dissociation) constant is $K_d = k_{off}/k_{on} = \kappa_d/(a\kappa_r)$, as in Eq. 1. The above expressions bridge between the diffusion-controlled limit, where k_D is small (then $k_{on} \approx k_D$ and $k_{off} \approx k_D K_d$), and the reaction-controlled limit, when k_D is large so that $k_{on} \approx a\kappa_r$ and $k_{off} \approx \kappa_d$. The rate parameters for the kinetic scheme (Eq. 7) are summarized in Table 5. The main message from this table is that $k_{on} = 24\ \mu\text{M}^{-1}\ \text{s}^{-1}$ emerging from the simulation is well within the acceptable range of binding rate parameters (e.g., see Clements and Westbrook, 1991).

DISCUSSION

The fundamental model of synaptic transmission

Simplified models can play an important role in the development of science, provided they capture the essential underlying physical behavior. The present work has considered a simplified ("fundamental") model for synaptic transmission, inasmuch as it ignores complicating effects of real experimental systems such as hydrolysis by AChE, desensitization of AMPA receptors, reuptake of glutamate, spillover between synapses, and details of the transmitter release process. Perhaps the most dramatic of our simplified assumptions involves ignoring receptor protein substates and focusing only on its binding states. Existing models assume at least closed and open substates for the (doubly) bound receptor state. In the present work, a doubly bound receptor is considered to have an open channel, implying that the closed → open transition is fast on the EPSC time scale.

Kinetic and approximate diffusion models, formulated in terms of average concentrations, do not treat basic concepts such as the role of transmitter rebinding in shaping the synaptic response (Katz and Miledi, 1973). Our simulations follow the history of every particle in the presence of a static array of reversible receptors, generating the binding states of the receptors in the array, which average to produce the

TABLE 5 Rate parameters for the kinetic scheme in Eq. 7 derived from the simulation parameters of Table 4

Bimolecular ($\mu\text{M}^{-1}\ \text{s}^{-1}$)		Unimolecular (s^{-1})	
k_D	34		
$a\kappa_r$	78	κ_d	750
k_{on}	24	k_{off}	230

overall synaptic response. Although such attributes may also be calculated using microscopic Monte Carlo simulations, these are less accurate in treating the reversible binding process. Our Brownian dynamics algorithm is based on experience gained from simulating reversible diffusion-influenced reactions in solution (Edelstein and Agmon, 1995). Its accuracy is due to the use of exact single-particle solutions for diffusion perpendicular to a reversible site (Edelstein and Agmon, 1997).

In the following discussion we focus on collective binding properties of receptor arrays, namely, the role of rebinding and spatial correlations of double-site receptors in shaping the synaptic signal (particularly its decay phase). We summarize the various geometric and kinetic parameters determining the relative magnitude of such effects. In particular, we relate our conclusions to the wealth of experimental data summarized in the Introduction.

Determinants of repetitive binding

We have found that under certain conditions rebinding determines the total number of particles bound to the array. The first factor that favors rebinding is the narrow width of the synaptic gap, which is typically comparable to the distance between receptors and much smaller than the distance from the release site to the extracellular pool. On a sufficiently long time scale, a transmitter particle resembles a photon bouncing between two mirrors: the pre- and postsynaptic membranes. It thus collides with each membrane many times and, if the array size (M) and receptor density are sufficiently large, it will encounter many receptors. Furthermore, if the receptor affinity is sufficiently high and a large fraction of the sites are empty, rebinding is bound to occur.

The first experimentally variable factor is the number of receptors in an array ($M/2$). For small M, rebinding probability is almost as small as for an isolated receptor, and we expect the kinetic properties of the array to resemble those of an isolated receptor in an O/O patch-clamp experiment. The fact that for NMDA receptors the EPSC time course is superimposable on the averaged single-receptor response (Lester and Jahr, 1992) and the evidence that NMDA EPSC is determined primarily by deactivation (Jonas and Sprusston, 1994) might simply indicate that the number of NMDA receptors in a typical CNS receptor array is very small. Indeed, experimental evidence shows that only a few (<5) NMDA receptors are colocalized with AMPA receptors in the postsynaptic array (Silver et al., 1992). Generalizing NMDA studies to conclude that rebinding is unimportant in the CNS is thus premature.

The correlation of synapse size with synapse efficacy in the CNS (Lisman and Harris, 1993) corroborates our conclusion. For AMPA receptors, both limiting cases of small and large M seem to have been observed. The small synapses formed by mossy fibers on small granule cells exhibit a fast (1 ms) mini-EPSC decay that matches single-receptor response (Silver et al., 1992), whereas the giant synapses on unipolar-brush cells reveal a super-slow decay phase of a few seconds (Rossi et al., 1995). In the NMJ, toxins that reduce the effective receptor density speed up EPC decay due to less frequent repetitive binding of ACh (Magleby and Terrar, 1975; Land et al., 1984; Giniatullin et al., 1993).

Another experimental variable is the number of transmitter particles (N). If $N \gg M$, the array saturates during the rising phase, as is believed to be the case in CNS synapses (Tang et al., 1994). The excess neurotransmitters ($N - M$) clear the gap very rapidly by diffusion. We find that the diffusion coefficient in the synaptic gap is about an order of magnitude lower than in solution, in qualitative agreement with diffusion measurements (Rice et al., 1985) and anatomical evidence (Ichimura and Hashimoto, 1988) for the tortuosity of diffusion paths in the synaptic gap. Yet even with this slower diffusional rate, most unbound particles will clear the gap within a fraction of a millisecond, in agreement with experimental determinations of the brief glutamate residence time in the synaptic cleft (Clements et al., 1992; Clements, 1996). As the remaining, bound particles start to dissociate and escape, the array coverage gradually decreases. Thus different behavior is expected during the early and late phases of the EPSC decay. During the early decay phase, the array is still close to saturation, so dissociated particles cannot rebind. During the late phase, array sites are mostly vacant, so dissociating particles rebind many times on their way out. This slows the late decay phase considerably, leading to nonexponential decay, as often observed experimentally. Although this slow phase is traditionally fitted by a second exponential, our results suggest that it is in fact hyperbolic. It would be interesting if sufficiently long EPSC tails could be measured to test this prediction.

Desensitization, which is typically 3–4 times slower than deactivation (Jonas and Spruston, 1994), is expected to mask the late decay phase. Rebinding, which still occurs, is simply not manifested in the EPSC decay. In systems where desensitization is incomplete (or when the experimental signal/noise ratio is favorable), a slow decay phase can indeed be observed (Otis et al., 1996). In other synapses, when desensitization is blocked (e.g., by CTZ), the late decay phase is unmasked (Yamada and Tang, 1993; Trussell et al., 1993; Diamoand and Jahr, 1995; Mennerick and Zorumski, 1995; Takahashi et al., 1995). Even if CTZ exerts additional effects, such as slowing deactivation (Patneau et al., 1993), these are not expected to add a second decay phase, as unmasking desensitization does. The fact that in the presence of CTZ, block of reuptake further prolongs the slow decay phase (Mennerick and Zorumski, 1995) suggests that multiple binding indeed takes place. In synapses that exhibit very slow decay, even in the presence of desensitization, uptake block selectively prolongs this late decay phase (Otis et al., 1996). Similarly in the NMJ, block of AChE activity prolongs the EPC decay by enhancing repetitive binding (Katz and Miledi, 1973; Hartzell et al., 1975; Magleby and Terrar, 1975; Kordaš, 1977; Land et al.,

1984; Magazanik et al., 1984; Giniatullin et al., 1993). Finally, our simulations, which reproduce AMPA EPSC decay of CTZ-treated hippocampal neurons with realistic geometric and kinetic parameters (previous section), clearly show that transmitter particles may rebind dozens of times before ultimately clearing the array zone. Taken together, these data present convincing evidence for the role of rebinding in shaping the late phase of EPSC decay.

The loss of spatial correlations

The effect of the number of transmitter molecules on the current decay is complicated by the fact that receptor activation requires double-site occupancy. Consider the case $N \ll M$ (an array is well below saturation), which probably holds for NMJ synapses (Hartzell et al., 1975). When N is very small, a rebinding agonist will land with high probability in a vacant receptor (converting it to the singly occupied state). Under low coverage conditions, rebinding is prominent but does not prolong the EPC decay. If N is larger (but still below saturation), a rebinding particle has a greater probability of landing in a singly occupied receptor. Here rebinding will prolong the decay phase, as seen in our "chessboard" simulations.

The above conclusions are in agreement with experimental evidence showing that under the influence of anticholinesterase, increasing the amount of transmitter released prolongs EPCs (Magleby and Terrar, 1975). Moreover, under conditions that enhance transmitter release in the NMJ, the duration of the EPC becomes considerably longer than that of a mini-EPC (Katz and Miledi, 1979; Magazanik et al., 1984; Giniatullin et al., 1993). Here the number of singly bound receptors might be sufficiently large that formation of doubly bound receptors by repetitive binding becomes nonnegligible. In contrast, for very small N, rebinding is predominantly to a nonbonded receptor, so there is no effect of varying N on the decay time constant. This might explain the critical quantum number required to see EPC prolongation (Giniatullin et al., 1993).

In a double-pulse experiment in the presence of anticholinesterase (Magazanik et al., 1984), the second EPC was both enhanced and prolonged as compared with the first EPC, even when the time spacing between stimuli was as large as 30 s, when the first EPC has decayed essentially to zero. The most consistent interpretation of this observation (Magazanik et al., 1984) is that singly bound ACh receptors, formed by (multiple cycles of) repetitive binding, persist for up to 30 s. This very slow time scale for transmitter removal by the "surface hopping" mechanism is consistent with the above-mentioned observation of EPSC decay of up to 3 s in giant unipolar-brush synapses (Rossi et al., 1995). The residence time of neurotransmitter in the synaptic cleft can actually be much longer than the duration of the synaptic current! For very large synapses in the absence of alternative signal-terminating processes (hydrolysis, desensitization, or reuptake), the decay reflects the loss of spatial correlations, converting doubly occupied receptors into pairs of singly occupied receptors. This explains the need for AChE in the NMJ, because large arrays might trap transmitter molecules "indefinitely" without the action of AChE.

We are grateful to Ariel Agmon for insightful remarks and help in the literature search. We thank Boris Barbour, David Colquhoun, Mark L. Mayer, Hana Parnas, and N. Traverse Slater for discussions and comments.

This work was supported in part by a grant from the Israel Science Foundation. The Fritz Haber Research Center is supported by the Minerva Gesellschaft für die Forschung (München, Germany).

REFERENCES

Agmon, N., and A. L. Edelstein. 1995. Geometric and many-particle aspects of transmitter binding. *Biophys. J.* 68:815–825.

Agmon, N., and A. Szabo. 1990. Theory of reversible diffusion-influenced reactions. *J. Chem. Phys.* 92:5270–5284.

Barbour, B., B. U. Keller, I. Llano, and A. Marty. 1994. Prolonged presence of glutamate during excitatory synaptic transmission to cerebellar Purkinje cells. *Neuron.* 12:1331–1343.

Bartol, T. M., Jr., B. R. Land, E. E. Salpeter, and M. M. Salpeter. 1991. Monte Carlo simulation of miniature endplate current generation in the vertebrate neuromuscular junction. *Biophys. J.* 59:1290–1307.

Becker, O. M., M. Silverberg, and A. Ben-Shaul. 1990. Kinetically controlled aggregation in reactive adsorbate overlayers. *Isr. J. Chem.* 30: 179–188.

Bekkers, J. M., and C. F. Stevens. 1989. NMDA and non-NMDA receptors are co-localized at individual excitatory synapses in cultured rat hippocampus. *Nature.* 341:230–233.

Clements, J. D. 1996. Transmitter timecourse in the synaptic cleft: its role in central synaptic function. *Trends Neurosci.* 19:163–171.

Clements, J. D., R. A. J. Lester, G. Tong, C. E. Jahr, and G. L. Westbrook. 1992. The time course of glutamate in the synaptic cleft. *Science.* 258:1498–1501.

Clements, J. D., and G. L. Westbrook. 1991. Activation kinetics reveal the number of glutamate and glycine binding sites on the *N*-methyl-D-aspartate receptor. *Neuron.* 7:605–613.

Diamond, J. S., and C. E. Jahr. 1995. Asynchronous release of synaptic vesicles determines the time course of the AMPA receptor-mediated EPSC. *Neuron.* 15:1097–1107.

Eccles, J. C., and J. C. Jaeger. 1958. The relationship between the mode of operation and the dimensions of the junctional regions at synapses and motor-end-organs. *Proc. R. Soc. Lond. B.* 148:38–56.

Edelstein, A. L., and N. Agmon. 1993. Brownian dynamics simulations of reversible reactions in one dimension. *J. Chem. Phys.* 99:5396–5404.

Edelstein, A. L., and N. Agmon. 1995. Equilibration in reversible bimolecular reactions. *J. Phys. Chem.* 99:5389–5401.

Edelstein, A. L., and N. Agmon. 1997. Brownian-simulation of many-particle binding to a reversible receptor array. *J. Comp. Phys.* 132: 000–000.

Edmonds, B., A. J. Gibb, and D. Colquhoun. 1995a. Mechanisms of activation of muscle nicotinic acetylcholine receptors and the time course of endplate currents. *Annu. Rev. Physiol.* 57:469–493.

Edmonds, B., A. J. Gibb, and D. Colquhoun. 1995b. Mechanisms of activation of glutamate receptors and the time course of excitatory synaptic currents. *Annu. Rev. Physiol.* 57:495–519.

Faber, D. S., W. S. Young, P. Legendre, and H. Korn. 1992. Intrinsic quantal variability due to stochastic properties of receptor-transmitter interactions. *Science.* 258:1494–1498.

Friboulet, A. and D. Thomas. 1993. Reaction-diffusion coupling in a structured system: application to the quantitative simulation of endplate currents. *J. Theor. Biol.* 160:441–455.

Giniatullin, R. A., R. N. Khazipov, and F. Vyskočil. 1993. A correlation between quantal content and decay time of endplate currents in frog muscles with intact cholinesterase. *J. Physiol. (Lond.).* 466:95–103.

Gogan, P., I. Schmiedel-Jakob, Y. Chitti, and S. Tyč-Dumont. 1995. Fluorescence imaging of local membrane electric fields during the excitation of single neurons in culture. *Biophys. J.* 69:299–310.

Gutman, M., E. Nachliel, and S. Kiryati. 1992. Dynamic studies of proton diffusion in mesoscopic heterogeneous matrix. II. The interbilayer space between phospholipid membranes. *Biophys. J.* 63:281–290.

Harris, K. M. and D. M. D. Landis. 1986. Membrane structure at synaptic junctions in area CA1 of the rat hippocampus. *Neuroscience.* 19: 857–872.

Hartzell, H. C., S. W. Kuffler, and D. Yoshikami. 1975. Post-synaptic potentiation: interaction between quanta of acetylcholine at the skeletal neuromuscular synapse. *J. Physiol. (Lond.).* 251:427–463.

Holmes, W. R. 1995. Modeling the effect of glutamate diffusion and uptake on NMDA and non-NMDA receptor saturation. *Biophys. J.* 69:1734–1747.

Ichimura, T., and P. H. Hashimoto. 1988. Structural components in the synaptic cleft captured by freeze-substitution and deep etching of directly frozen cerebellar cortex. *J. Neurocytol.* 17:3–12.

Isaacson, J. S., and B. Walmsley. 1995. Counting quanta: direct measurements of transmitter release at a central synapse. *Neuron.* 15:875–884.

Jonas, P., and N. Spruston. 1994. Mechanisms shaping glutamate-mediated excitatory postsynaptic currents in the CNS. *Curr. Opin. Neurobiol.* 4:366–372.

Katz, B., and R. Miledi. 1973. The binding of acetylcholine to receptors and its removal from the synaptic cleft. *J. Physiol. (Lond.).* 231: 549–574.

Katz, B., and R. Miledi. 1979. Estimates of quantal content during "chemical potentiation" of transmitter release. *Proc. R. Soc. Lond. B.* 205: 369–378.

Kleinle, J., K. Vogt, H.-R. Lüscher, L. Müller, W. Senn, K. Wyler, and J. Streit. 1996. Transmitter concentration profiles in the synaptic cleft: an analytical model of release and diffusion. *Biophys. J.* 71:2413–2426.

Kordaš, M. 1977. On the role of junctional cholinesterase in determining the time course of the end-plate current. *J. Physiol. (Lond.).* 270: 133–150.

Korn, H., and D. S. Faber. 1991. Quantal analysis and synaptic efficacy in the CNS. *Trends Neurosci.* 14:439–445.

Land, B. R., W. V. Harris, E. E. Salpeter, and M. M. Salpeter. 1984. Diffusion and binding constants for acetylcholine derived from the falling phase of miniature endplate currents. *Proc. Natl. Acad. Sci. USA.* 81:1594–1598.

Land, B. R., E. E. Salpeter, and M. M. Salpeter. 1981. Kinetic parameters for acetylcholine interaction in intact neuromuscular junction. *Proc. Natl. Acad. Sci. USA.* 78:7200–7204.

Lester, R. A. J., J. D. Clements, G. L. Westbrook, and C. E. Jahr. 1990. Channel kinetics determine the time course of NMDA receptor-mediated synaptic currents. *Nature.* 346:565–567.

Lester, R. A. J., and C. E. Jahr. 1992. NMDA channel behavior depends on agonist affinity. *J. Neurosci.* 12:635–643.

Lisman, J. E., and K. M. Harris. 1993. Quantal analysis and synaptic anatomy—integrating two views of hippocampal plasticity. *Trends Neurosci.* 16:141–147.

Longworth, L. G. 1953. Diffusion measurements, at 25°, of aqueous solutions of amino acids, peptides and sugars. *J. Am. Chem. Soc.* 75:5705–5709.

Magazanik, L. G., E. E. Nikolsky, and R. A. Giniatullin. 1984. End-plate currents evoked by paired stimuli in frog muscle fibres. *Pflügers Arch.* 401:185–192.

Magleby, K. L., and C. F. Stevens. 1972. A quantitative description of end-plate currents. *J. Physiol. (Lond.).* 223:173–197.

Magleby, K. L., and D. A. Terrar. 1975. Factors affecting the time course of decay of end-plate currents: a possible cooperative action of acetylcholine on receptors at the frog neuromuscular junction. *J. Physiol. (Lond.).* 244:467–495.

Matthews-Bellinger, J., and M. M. Salpeter. 1978. Distribution of acetylcholine receptors at frog neuromuscular junction with a discussion of some physiological implications. *J. Physiol. (Lond.).* 279:197–213.

Mennerick, S., and C. F. Zorumski. 1995. Presynaptic influence on the time course of fast excitatory synaptic currents in cultured hippocampal cells. *J. Neurosci.* 15:3178–3192.

Nicholson, C., and J. M. Phillips. 1981. Ion diffusion modified by tortuosity and volume fraction in the extracellular microenvironment of the rat cerebellum. *J. Physiol. (Lond.).* 321:225–257.

Otis, T. S., Y.-C. Wu, and L. O. Trussell. 1996. Delayed clearance of transmitter and the role of glutamate transporters at synapses with multiple release sites. *J. Neurosci.* 16:1634–1644.

Parnas, H., M. Flashner, and M. E. Spira. 1989. Sequential model to describe the nicotinic synaptic current. *Biophys. J.* 55:875–884.

Patneau, D. K., and M. L. Mayer. 1990. Structure-activity relationships for amino acid transmitter candidates acting at *N*-methyl-D-aspartate and quisqualate receptors. *J. Neurosci.* 10:2385–2399.

Patneau, D. K., L. Vyklicky, Jr., and M. L. Mayer. 1993. Hippocampal neurons exhibit cyclothiazide-sensitive rapidly desensitizing responses to kainate. *J. Neurosci.* 13:3496–3509.

Rice, M. E., G. A. Gerhardt, P. M. Hierl, G. Nagy, and R. N. Adams. 1985. Diffusion coefficients of neurotransmitters and their metabolites in brain extracellular fluid space. *Neuroscience.* 15:891–902.

Rosenberry, T. 1979. Quantitative simulation of endplate currents at neuromuscular junctions based on the reaction of acetylcholine with acetylcholine receptor and acetylcholinesterase. *Biophys. J.* 26:263–290.

Rossi, D. J., S. Alford, E. Mugnaini, and N. T. Slater. 1995. Properties of transmission at a giant glutamatergic synapse in cerebellum: the mossy fiber-unipolar brush cell synapse. *J. Neurophysiol.* 74:24–42.

Shoup, D., and A. Szabo. 1982. Role of diffusion in ligand binding to macromolecules and cell-bound receptors. *Biophys. J.* 40:33–39.

Silver, R. A., D. Colquhoun, S. G. Cull-Candy, and B. Edmonds. 1996. Deactivation and desensitization of non-NMDA receptors in patches and the time course of EPSCs in rat cerebellar granule cells. *J. Physiol. (Lond.).* 493:167–173.

Silver, R. A., S. F. Traynelis, and S. G. Cull-Candy. 1992. Rapid-time course miniature and evoked excitatory currents at cerebellar synapses in situ. *Nature.* 355:163–166.

Takahashi, M., Y. Kovalchuk, and D. Attwell. 1995. Pre- and postsynaptic determinants of EPSC waveform at cerebellar climbing fiber and parallel fiber to Purkinje cell synapses. *J. Neurosci.* 15:5693–5702.

Tang, C.-M., M. Margulis, Q.-Y. Shi, and A. Fielding. 1994. Saturation of postsynaptic glutamate receptors after quantal release of transmitter. *Neuron.* 13:1385–1393.

Tong, G., and C. E. Jahr. 1994. Block of glutamate transporters potentiates postsynaptic excitation. *Neuron.* 13:1195–1203.

Trussell, L. O., S. Zhang, and I. M. Raman. 1993. Desensitization of AMPA receptors upon multiquantal neurotransmitter release. *Neuron.* 10:1185–1196.

Uteshev, V. V., and P. S. Pennefather. 1996. A mathematical description of miniature postsynaptic current generation at central nervous system synapses. *Biophys. J.* 71:1256–1266.

Vyklicky, L., Jr., D. K. Patneau, and M. L. Mayer. 1991. Modulation of excitatory synaptic transmission by drugs that reduce desensitization at AMPA/kainte receptors. *Neuron.* 7:971–984.

Wahl, L. M., C. Pouzat, and K. J. Stratford. 1996. Monte carlo simulations of fast excitatory synaptic transmission at the hipocampal synapse. *J. Neurophysiol.* 75:597–608.

Wathey, J. C., M. M. Nass, and H. A. Lester. 1979. Numerical reconstruction of the quantal event at nicotinic synapses. *Biophys. J.* 27:145–164.

Yamada, K. A., and C.-M. Tang. 1993. Benzothiadiazides inhibit rapid glutamate receptor desensitization and enhance glutamatergic synaptic currents. *J. Neurosci.* 13:3904–3915.